Third Edition

Sponsored by the Optical Society of America

HANDBOOK OF OPTICS

Volume V

Atmospheric Optics, Modulators, Fiber Optics, X-Ray and Neutron Optics

Editor-in-Chief:
Michael Bass

Associate Editors:
Casimer M. DeCusatis
Jay M. Enoch
Vasudevan Lakshminarayanan
Guifang Li
Carolyn MacDonald
Virendra N. Mahajan
Eric Van Stryland

OSA

SPERO EX. 2060

HANDBOOK OF OPTICS

SPERO EX. 2060

ABOUT THE EDITORS

Editor-in-Chief: Dr. Michael Bass is professor emeritus at CREOL, The College of Optics and Photonics, University of Central Florida, Orlando, Florida.

Associate Editors:
Dr. Casimer M. DeCusatis is a distinguished engineer and technical executive with IBM Corporation, Poughkeepsie, New York.

Dr. Jay M. Enoch is dean emeritus and professor at the School of Optometry at the University of California, Berkeley.

Dr. Vasudevan Lakshminarayanan is professor of Optometry, Physics, and Electrical Engineering at the University of Waterloo, Ontario, Canada.

Dr. Guifang Li is a professor at CREOL, The College of Optics and Photonics, University of Central Florida, Orlando, Florida.

Dr. Carolyn MacDonald is professor and chair of physics at the University at Albany, SUNY, and the director of the Albany Center for X-Ray Optics.

Dr. Virendra N. Mahajan is a distinguished scientist at The Aerospace Corporation.

Dr. Eric Van Stryland is a professor at CREOL, The College of Optics and Photonics, University of Central Florida, Orlando, Florida.

SPERO EX. 2060

HANDBOOK OF OPTICS

Volume V

Atmospheric Optics, Modulators, Fiber Optics, X-Ray and Neutron Optic

THIRD EDITION

Sponsored by the
OPTICAL SOCIETY OF AMERICA

Michael Bass Editor-in-Chief

CREOL, The College of Optics and Photonics
University of Central Florida
Orlando, Florida

Carolyn MacDonald Associate Editor

Department of Physics
University at Albany
Albany, New York

Guifang Li Associate Editor

CREOL, The College of Optics and Photonics
University of Central Florida
Orlando, Florida

Casimer M. DeCusatis Associate Editor

IBM Corporation
Poughkeepsie, New York

Virendra N. Mahajan Associate Editor

Aerospace Corporation
El Segundo, California

New York Chicago San Francisco Lisbon London Madrid
Mexico City Milan New Delhi San Juan Seoul
Singapore Sydney Toronto

SPERO EX. 2060

The McGraw·Hill Companies

Copyright © 2010 by The McGraw-Hill Companies, Inc. All rights reserved. Except as permitted under the United States Copyright Act of 1976, no part of this publication may be reproduced or distributed in any form or by any means, or stored in a database or retrieval system, without the prior written permission of the publisher.

ISBN: 978-0-07-163314-7

MHID: 0-07-163314-6

The material in this eBook also appears in the print version of this title: ISBN: 978-0-07-163313-0, MHID: 0-07-163313-8.

All trademarks are trademarks of their respective owners. Rather than put a trademark symbol after every occurrence of a trademarked name, we use names in an editorial fashion only, and to the benefit of the trademark owner, with no intention of infringement of the trademark. Where such designations appear in this book, they have been printed with initial caps.

McGraw-Hill eBooks are available at special quantity discounts to use as premiums and sales promotions, or for use in corporate training programs. To contact a representative please e-mail us at bulksales@mcgraw-hill.com.

Information contained in this work has been obtained by The McGraw-Hill Companies, Inc. (“McGraw-Hill”) from sources believed to be reliable. However, neither McGraw-Hill nor its authors guarantee the accuracy or completeness of any information published herein, and neither McGraw-Hill nor its authors shall be responsible for any errors, omissions, or damages arising out of use of this information. This work is published with the understanding that McGraw-Hill and its authors are supplying information but are not attempting to render engineering or other professional services. If such services are required, the assistance of an appropriate professional should be sought.

TERMS OF USE

This is a copyrighted work and The McGraw-Hill Companies, Inc. (“McGraw-Hill”) and its licensors reserve all rights in and to the work. Use of this work is subject to these terms. Except as permitted under the Copyright Act of 1976 and the right to store and retrieve one copy of the work, you may not decompile, disassemble, reverse engineer, reproduce, modify, create derivative works based upon, transmit, distribute, disseminate, sell, publish or sublicense the work or any part of it without McGraw-Hill’s prior consent. You may use the work for your own noncommercial and personal use; any other use of the work is strictly prohibited. Your right to use the work may be terminated if you fail to comply with these terms.

THE WORK IS PROVIDED “AS IS.” McGRAW-HILL AND ITS LICENSORS MAKE NO GUARANTEES OR WARRANTIES AS TO THE ACCURACY, ADEQUACY OR COMPLETENESS OF OR RESULTS TO BE OBTAINED FROM USING THE WORK, INCLUDING ANY INFORMATION THAT CAN BE ACCESSED THROUGH THE WORK VIA HYPERLINK OR OTHERWISE, AND EXPRESSLY DISCLAIM ANY WARRANTY, EXPRESS OR IMPLIED, INCLUDING BUT NOT LIMITED TO IMPLIED WARRANTIES OF MERCHANTABILITY OR FITNESS FOR A PARTICULAR PURPOSE. McGraw-Hill and its licensors do not warrant or guarantee that the functions contained in the work will meet your requirements or that its operation will be uninterrupted or error free. Neither McGraw-Hill nor its licensors shall be liable to you or anyone else for any inaccuracy, error or omission, regardless of cause, in the work or for any damages resulting therefrom. McGraw-Hill has no responsibility for the content of any information accessed through the work. Under no circumstances shall McGraw-Hill and/or its licensors be liable for any indirect, incidental, special, punitive, consequential or similar damages that result from the use of or inability to use the work, even if any of them has been advised of the possibility of such damages. This limitation of liability shall apply to any claim or cause whatsoever whether such claim or cause arises in contract, tort or otherwise.

SPERO EX. 2060

COVER ILLUSTRATIONS

Boadband supercontinuum. Generated in a photonic crystal fiber using a mode-locked Ti:Sapphire laser as pump source. The spectrum is much broader than seen in the photograph, extending from 400 nm to beyond 2 μm. (*Photo courtesy of the Optoelectronics Group, University of Bath.*)

Supernova remnant. A Chandra X-Ray Space Telescope image of the supernova remnant G292.0+1.8. The colors in the image encode the X-ray energies emitted by the supernova remnant; the center of G292.0+1.8 contains a region of high energy X-ray emission from the magnetized bubble of high-energy particles that surrounds the pulsar, a rapidly rotating neutron star that remained behind after the original, massive star exploded. (*This image is from NASA/CXC/Penn State/S.Park et al. and more detailed information can be found on the Chandra website: http://chandra.harvard.edu/photo/2007/g292/.*)

Crab Nebula. A Chandra X-Ray Space Telescope image of the Crab Nebula—the remains of a nearby supernova explosion first seen on Earth in 1054 AD. At the center of the bright nebula is a rapidly spinning neutron star, or pulsar, that emits pulses of radiation 30 times a second. (*This image is from NASA/CXC/ASU/J.Hester et al. and more detailed information can be found on the Chandra website: http://chandra.harvard.edu/photo/2002/0052/.*)

SPERO EX. 2060

This page intentionally left blank

CONTENTS

Contributors xix
Brief Contents of All Volumes xxiii
Editors' Preface xxix
Preface to Volume V xxxi
Glossary and Fundamental Constants xxxiii

Part 1. Measurements

Chapter 1. Scatterometers *John C. Stover* 1.3

1.1 Glossary / *1.3*
1.2 Introduction / *1.3*
1.3 Definitions and Specifications / *1.5*
1.4 Instrument Configurations and Component Descriptions / *1.7*
1.5 Instrumentation Issues / *1.11*
1.6 Measurement Issues / *1.13*
1.7 Incident Power Measurement, System Calibration, and Error Analysis / *1.14*
1.8 Summary / *1.16*
1.9 References / *1.16*

Chapter 2. Spectroscopic Measurements *Brian Henderson* 2.1

2.1 Glossary / *2.1*
2.2 Introductory Comments / *2.2*
2.3 Optical Absorption Measurements of Energy Levels / *2.2*
2.4 The Homogeneous Lineshape of Spectra / *2.13*
2.5 Absorption, Photoluminescence, and Radiative Decay Measurements / *2.19*
2.6 References / *2.24*

Part 2. Atmospheric Optics

Chapter 3. Atmospheric Optics *Dennis K. Killinger, James H. Churnside, and Laurence S. Rothman* 3.3

3.1 Glossary / *3.3*
3.2 Introduction / *3.4*
3.3 Physical and Chemical Composition of the Standard Atmosphere / *3.6*
3.4 Fundamental Theory of Interaction of Light with the Atmosphere / *3.11*
3.5 Prediction of Atmospheric Optical Transmission: Computer Programs and Databases / *3.22*
3.6 Atmospheric Optical Turbulence / *3.26*
3.7 Examples of Atmospheric Optical Remote Sensing / *3.36*
3.8 Meteorological Optics / *3.40*
3.9 Atmospheric Optics and Global Climate Change / *3.43*
3.10 Acknowledgments / *3.45*
3.11 References / *3.45*

SPERO EX. 2060

Chapter 4. Imaging through Atmospheric Turbulence *Virendra N. Mahajan and Guang-ming Dai* 4.1

Abstract / *4.1*
4.1 Glossary / *4.1*
4.2 Introduction / *4.2*
4.3 Long-Exposure Image / *4.3*
4.4 Kolmogorov Turbulence and Atmospheric Coherence Length / *4.7*
4.5 Application to Systems with Annular Pupils / *4.10*
4.6 Modal Expansion of Aberration Function / *4.17*
4.7 Covariance and Variance of Expansion Coefficients / *4.20*
4.8 Angle of Arrival Fluctuations / *4.23*
4.9 Aberration Variance and Approximate Strehl Ratio / *4.27*
4.10 Modal Correction of Atmospheric Turbulence / *4.28*
4.11 Short-Exposure Image / *4.31*
4.12 Adaptive Optics / *4.35*
4.13 Summary / *4.36*
4.14 Acknowledgments / *4.37*
4.15 References / *4.37*

Chapter 5. Adaptive Optics *Robert Q. Fugate* 5.1

5.1 Glossary / *5.1*
5.2 Introduction / *5.2*
5.3 The Adaptive Optics Concept / *5.2*
5.4 The Nature of Turbulence and Adaptive Optics Requirements / *5.5*
5.5 AO Hardware and Software Implementation / *5.21*
5.6 How to Design an Adaptive Optical System / *5.38*
5.7 Acknowledgments / *5.46*
5.8 References / *5.47*

PART 3. Modulators

Chapter 6. Acousto-Optic Devices *I-Cheng Chang* 6.1

6.1 Glossary / *6.3*
6.2 Introduction / *6.4*
6.3 Theory of Acousto-Optic Interaction / *6.5*
6.4 Acousto-Optic Materials / *6.16*
6.5 Acousto-Optic Deflector / *6.22*
6.6 Acousto-Optic Modulator / *6.31*
6.7 Acousto-Optic Tunable Filter / *6.35*
6.8 References / *6.45*

Chapter 7. Electro-Optic Modulators *Georgeanne M. Purvinis and Theresa A. Maldonado* 7.1

7.1 Glossary / *7.1*
7.2 Introduction / *7.3*
7.3 Crystal Optics and the Index Ellipsoid / *7.3*
7.4 The Electro-Optic Effect / *7.6*
7.5 Modulator Devices / *7.16*
7.6 Applications / *7.36*
7.7 Appendix: Euler Angles / *7.39*
7.8 References / *7.40*

Chapter 8. Liquid Crystals *Sebastian Gauza and Shin-Tson Wu* 8.1

Abstract / *8.1*
8.1 Glossary / *8.1*

SPERO EX. 2060

8.2 Introduction to Liquid Crystals / *8.2*
8.3 Types of Liquid Crystals / *8.4*
8.4 Liquid Crystals Phases / *8.8*
8.5 Physical Properties / *8.13*
8.6 Liquid Crystal Cells / *8.25*
8.7 Liquid Crystals Displays / *8.29*
8.8 Polymer/Liquid Crystal Composites / *8.36*
8.9 Summary / *8.37*
8.10 References / *8.38*
8.11 Bibliography / *8.39*

Part 4. Fiber Optics

Chapter 9. Optical Fiber Communication Technology and System Overview *Ira Jacobs* 9.3

9.1 Introduction / *9.3*
9.2 Basic Technology / *9.4*
9.3 Receiver Sensitivity / *9.8*
9.4 Bit Rate and Distance Limits / *9.12*
9.5 Optical Amplifiers / *9.13*
9.6 Fiber-Optic Networks / *9.14*
9.7 Analog Transmission on Fiber / *9.15*
9.8 Technology and Applications Directions / *9.17*
9.9 References / *9.17*

Chapter 10. Nonlinear Effects in Optical Fibers *John A. Buck* 10.1

10.1 Key Issues in Nonlinear Optics in Fibers / *10.1*
10.2 Self- and Cross-Phase Modulation / *10.3*
10.3 Stimulated Raman Scattering / *10.4*
10.4 Stimulated Brillouin Scattering / *10.7*
10.5 Four-Wave Mixing / *10.9*
10.6 Conclusion / *10.11*
10.7 References / *10.12*

Chapter 11. Photonic Crystal Fibers *Philip St. J. Russell and Greg J. Pearce* 11.1

11.1 Glossary / *11.1*
11.2 Introduction / *11.2*
11.3 Brief History / *11.2*
11.4 Fabrication Techniques / *11.4*
11.5 Modeling and Analysis / *11.6*
11.6 Characteristics of Photonic Crystal Cladding / *11.7*
11.7 Linear Characteristics of Guidance / *11.11*
11.8 Nonlinear Characteristics of Guidance / *11.22*
11.9 Intrafiber Devices, Cutting, and Joining / *11.26*
11.10 Conclusions / *11.28*
11.11 Appendix / *11.28*
11.12 References / *11.28*

Chapter 12. Infrared Fibers *James A. Harrington* 12.1

12.1 Introduction / *12.1*
12.2 Nonoxide and Heavy-Metal Oxide Glass IR Fibers / *12.3*
12.3 Crystalline Fibers / *12.7*
12.4 Hollow Waveguides / *12.10*
12.5 Summary and Conclusions / *12.13*
12.6 References / *12.13*

SPERO EX. 2060

Chapter 13. Sources, Modulators, and Detectors for Fiber Optic Communication Systems *Elsa Garmire* 13.1

13.1 Introduction / *13.1*
13.2 Double Heterostructure Laser Diodes / *13.3*
13.3 Operating Characteristics of Laser Diodes / *13.8*
13.4 Transient Response of Laser Diodes / *13.13*
13.5 Noise Characteristics of Laser Diodes / *13.18*
13.6 Quantum Well and Strained Lasers / *13.24*
13.7 Distributed Feedback and Distributed Bragg Reflector Lasers / *13.28*
13.8 Tunable Lasers / *13.32*
13.9 Light-Emitting Diodes / *13.36*
13.10 Vertical Cavity Surface-Emitting Lasers / *13.42*
13.11 Lithium Niobate Modulators / *13.48*
13.12 Electroabsorption Modulators / *13.55*
13.13 Electro-Optic and Electrorefractive Modulators / *13.61*
13.14 *PIN* Diodes / *13.63*
13.15 Avalanche Photodiodes, MSM Detectors, and Schottky Diodes / *13.71*
13.16 References / *13.74*

Chapter 14. Optical Fiber Amplifiers *John A. Buck* 14.1

14.1 Introduction / *14.1*
14.2 Rare-Earth-Doped Amplifier Configuration and Operation / *14.2*
14.3 EDFA Physical Structure and Light Interactions / *14.4*
14.4 Other Rare-Earth Systems / *14.7*
14.5 Raman Fiber Amplifiers / *14.8*
14.6 Parametric Amplifiers / *14.10*
14.7 References / *14.11*

Chapter 15. Fiber Optic Communication Links (Telecom, Datacom, and Analog) *Casimer DeCusatis and Guifang Li* 15.1

15.1 Figures of Merit / *15.2*
15.2 Link Budget Analysis: Installation Loss / *15.6*
15.3 Link Budget Analysis: Optical Power Penalties / *15.8*
15.4 References / *15.18*

Chapter 16. Fiber-Based Couplers *Daniel Nolan* 16.1

16.1 Introduction / *16.1*
16.2 Achromaticity / *16.3*
16.3 Wavelength Division Multiplexing / *16.4*
16.4 $1 \times N$ Power Splitters / *16.4*
16.5 Switches and Attenuators / *16.4*
16.6 Mach-Zehnder Devices / *16.4*
16.7 Polarization Devices / *16.5*
16.8 Summary / *16.6*
16.9 References / *16.6*

Chapter 17. Fiber Bragg Gratings *Kenneth O. Hill* 17.1

17.1 Glossary / *17.1*
17.2 Introduction / *17.1*
17.3 Photosensitivity / *17.2*
17.4 Properties of Bragg Gratings / *17.3*
17.5 Fabrication of Fiber Gratings / *17.4*
17.6 The Application of Fiber Gratings / *17.8*
17.7 References / *17.9*

SPERO EX. 2060

Chapter 18. Micro-Optics-Based Components for Networking *Joseph C. Palais* 18.1

18.1 Introduction / *18.1*
18.2 Generalized Components / *18.1*
18.3 Network Functions / *18.2*
18.4 Subcomponents / *18.5*
18.5 Components / *18.9*
18.6 References / *18.12*

Chapter 19. Semiconductor Optical Amplifiers *Jay M. Wiesenfeld and Leo H. Spiekman* 19.1

19.1 Introduction / *19.1*
19.2 Device Basics / *19.2*
19.3 Fabrication / *19.15*
19.4 Device Characterization / *19.17*
19.5 Applications / *19.22*
19.6 Amplification of Signals / *19.22*
19.7 Switching and Modulation / *19.28*
19.8 Nonlinear Applications / *19.29*
19.9 Final Remarks / *19.36*
19.10 References / *19.36*

Chapter 20. Optical Time-Division Multiplexed Communication Networks *Peter J. Delfyett* 20.1

20.1 Glossary / *20.1*
20.2 Introduction / *20.3*
20.3 Multiplexing and Demultiplexing / *20.3*
20.4 Introduction to Device Technology / *20.12*
20.5 Summary and Future Outlook / *20.24*
20.6 Bibliography / *20.25*

Chapter 21. WDM Fiber-Optic Communication Networks *Alan E. Willner, Changyuan Yu, Zhongqi Pan, and Yong Xie* 21.1

21.1 Introduction / *21.1*
21.2 Basic Architecture of WDM Networks / *21.4*
21.3 Fiber System Impairments / *21.13*
21.4 Optical Modulation Formats for WDM Systems / *21.27*
21.5 Optical Amplifiers in WDM Networks / *21.37*
21.6 Summary / *21.44*
21.7 Acknowledgments / *21.44*
21.8 References / *21.44*

Chapter 22. Solitons in Optical Fiber Communication Systems *Pavel V. Mamyshev* 22.1

22.1 Introduction / *22.1*
22.2 Nature of the Classical Soliton / *22.2*
22.3 Properties of Solitons / *22.4*
22.4 Classical Soliton Transmission Systems / *22.5*
22.5 Frequency-Guiding Filters / *22.7*
22.6 Sliding Frequency-Guiding Filters / *22.8*
22.7 Wavelength Division Multiplexing / *22.9*
22.8 Dispersion-Managed Solitons / *22.12*
22.9 Wavelength-Division Multiplexed Dispersionmanaged Soliton Transmission / *22.15*
22.10 Conclusion / *22.17*
22.11 References / *22.17*

SPERO EX. 2060

Chapter 23. Fiber-Optic Communication Standards
Casimer DeCusatis 23.1

23.1 Introduction / *23.1*
23.2 ESCON / *23.1*
23.3 FDDI / *23.2*
23.4 Fibre Channel Standard / *23.4*
23.5 ATM/SONET / *23.6*
23.6 Ethernet / *23.7*
23.7 Infiniband / *23.8*
23.8 References / *23.8*

Chapter 24. Optical Fiber Sensors *Richard O. Claus, Ignacio Matias, and Francisco Arregui* 24.1

24.1 Introduction / *24.1*
24.2 Extrinsic Fabry-Perot Interferometric Sensors / *24.2*
24.3 Intrinsic Fabry-Perot Interferometric Sensors / *24.4*
24.4 Fiber Bragg Grating Sensors / *24.5*
24.5 Long-Period Grating Sensors / *24.8*
24.6 Comparison of Sensing Schemes / *24.13*
24.7 Conclusion / *24.13*
24.8 References / *24.13*
24.9 Further Reading / *24.14*

Chapter 25. High-Power Fiber Lasers and Amplifiers
Timothy S. McComb, Martin C. Richardson, and Michael Bass 25.1

25.1 Glossary / *25.1*
25.2 Introduction / *25.3*
25.3 Fiber Laser Limitations / *25.6*
25.4 Fiber Laser Fundamentals / *25.7*
25.5 Fiber Laser Architectures / *25.9*
25.6 LMA Fiber Designs / *25.18*
25.7 Active Fiber Dopants / *25.22*
25.8 Fiber Fabrication and Materials / *25.26*
25.9 Spectral and Temporal Modalities / *25.29*
25.10 Conclusions / *25.33*
25.11 References / *25.33*

PART 5. X-Ray and Neutron Optics

SUBPART 5.1. INTRODUCTION AND APPLICATIONS

Chapter 26. An Introduction to X-Ray and Neutron Optics
Carolyn MacDonald 26.5

26.1 History / *26.5*
26.2 X-Ray Interaction with Matter / *26.6*
26.3 Optics Choices / *26.7*
26.4 Focusing and Collimation / *26.9*
26.5 References / *26.11*

Chapter 27. Coherent X-Ray Optics and Microscopy *Qun Shen* 27.1

27.1 Glossary / *27.1*
27.2 Introduction / *27.2*
27.3 Fresnel Wave Propagation / *27.2*
27.4 Unified Approach for Near- and Far-Field Diffraction / *27.2*

SPERO EX. 2060

27.5 Coherent Diffraction Microscopy / *27.4*
27.6 Coherence Preservation in X-Ray Optics / *27.5*
27.7 References / *27.5*

Chapter 28. Requirements for X-Ray Diffraction *Scott T. Misture* 28.1

28.1 Introduction / *28.1*
28.2 Slits / *28.1*
28.3 Crystal Optics / *28.3*
28.4 Multilayer Optics / *28.5*
28.5 Capillary and Polycapillary Optics / *28.5*
28.6 Diffraction and Fluorescence Systems / *28.5*
28.7 X-Ray Sources and Microsources / *28.7*
28.8 References / *28.7*

Chapter 29. Requirements for X-Ray Fluorescence *Walter Gibson and George* Havrilla 29.1

29.1 Introduction / *29.1*
29.2 Wavelength-Dispersive X-Ray Fluorescence (WDXRF) / *29.2*
29.3 Energy-Dispersive X-Ray Fluorescence (EDXRF) / *29.3*
29.4 References / *29.12*

Chapter 30. Requirements for X-Ray Spectroscopy *Dirk Lützenkirchen-Hecht and Ronald Frahm* 30.1

30.1 References / *30.5*

Chapter 31. Requirements for Medical Imaging and X-Ray Inspection *Douglas Pfeiffer* 31.1

31.1 Introduction to Radiography and Tomography / *31.1*
31.2 X-Ray Attenuation and Image Formation / *31.1*
31.3 X-Ray Detectors and Image Receptors / *31.4*
31.4 Tomography / *31.5*
31.5 Computed Tomography / *31.5*
31.6 Digital Tomosynthesis / *31.7*
31.7 Digital Displays / *31.8*
31.8 Conclusion / *31.9*
31.9 References / *31.10*

Chapter 32. Requirements for Nuclear Medicine *Lars R. Furenlid* 32.1

32.1 Introduction / *32.1*
32.2 Projection Image Acquisition / *32.2*
32.3 Information Content in SPECT / *32.3*
32.4 Requirements for Optics For SPECT / *32.4*
32.5 References / *32.4*

Chapter 33. Requirements for X-Ray Astronomy *Scott O. Rohrbach* 33.1

33.1 Introduction / *33.1*
33.2 Trade-Offs / *33.2*
33.3 Summary / *33.4*

Chapter 34. Extreme Ultraviolet Lithography *Franco Cerrina and Fan Jiang* 34.1

34.1 Introduction / *34.1*
34.2 Technology / *34.2*

SPERO EX. 2060

34.3 Outlook / *34.5*
34.4 Acknowledgments / *34.6*
34.5 References / *34.7*

Chapter 35. Ray Tracing of X-Ray Optical Systems *Franco Cerrina and Manuel Sanchez del Rio* 35.1

35.1 Introduction / *35.1*
35.2 The Conceptual Basis of SHADOW / *35.2*
35.3 Interfaces and Extensions of SHADOW / *35.3*
35.4 Examples / *35.4*
35.5 Conclusions and Future / *35.5*
35.6 References / *35.6*

Chapter 36. X-Ray Properties of Materials *Eric M. Gullikson* 36.1

36.1 X-Ray and Neutron Optics / *36.2*
36.2 Electron Binding Energies, Principal K- and L-Shell Emission Lines, and Auger Electron Energies / *36.3*
36.3 References / *36.10*

SUBPART 5.2. REFRACTIVE AND INTERFERENCE OPTICS

Chapter 37. Refractive X-Ray Lenses *Bruno Lengeler and Christian G. Schroer* 37.3

37.1 Introduction / *37.3*
37.2 Refractive X-Ray Lenses with Rotationally Parabolic Profile / *37.4*
37.3 Imaging with Parabolic Refractive X-Ray Lenses / *37.6*
37.4 Microfocusing with Parabolic Refractive X-Ray Lenses / *37.7*
37.5 Prefocusing and Collimation with Parabolic Refractive X-Ray Lenses / *37.8*
37.6 Nanofocusing Refractive X-Ray Lenses / *37.8*
37.7 Conclusion / *37.11*
37.8 References / *37.11*

Chapter 38. Gratings and Monochromators in the VUV and Soft X-Ray Spectral Region *Malcolm R. Howells* 38.1

38.1 Introduction / *38.1*
38.2 Diffraction Properties / *38.1*
38.3 Focusing Properties / *38.3*
38.4 Dispersion Properties / *38.6*
38.5 Resolution Properties / *38.7*
38.6 Efficiency / *38.8*
38.7 References / *38.8*

Chapter 39. Crystal Monochromators and Bent Crystals *Peter Siddons* 39.1

39.1 Crystal Monochromators / *39.1*
39.2 Bent Crystals / *39.5*
39.3 References / *39.6*

Chapter 40. Zone Plates *Alan Michette* 40.1

40.1 Introduction / *40.1*
40.2 Geometry of a Zone Plate / *40.1*
40.3 Zone Plates as Thin Lenses / *40.3*
40.4 Diffraction Efficiencies of Zone Plates / *40.4*
40.5 Manufacture of Zone Plates / *40.8*

SPERO EX. 2060

40.6 Bragg-Fresnel Lenses / *40.9*
40.7 References / *40.10*

Chapter 41. Multilayers *Eberhard Spiller* 41.1

41.1 Glossary / *41.1*
41.2 Introduction / *41.1*
41.3 Calculation of Multilayer Properties / *41.3*
41.4 Fabrication Methods and Performance / *41.4*
41.5 Multilayers for Diffractive Imaging / *41.9*
41.6 References / *41.10*

Chapter 42. Nanofocusing of Hard X-Rays with Multilayer Laue Lenses *Albert T. Macrander, Hanfei Yan, Hyon Chol Kang, Jörg Maser, Chian Liu, Ray Conley, and G. Brian Stephenson* 42.1

Abstract / *42.1*
42.1 Introduction / *42.2*
42.2 MLL Concept and Volume Diffraction Calculations / *42.4*
42.3 Magnetron-Sputtered MLLs / *42.5*
42.4 Instrumental Beamline Arrangement and Measurements / *42.9*
42.5 Takagi-Taupin Calculations / *42.12*
42.6 Wedged MLLs / *42.12*
42.7 MMLs with Curved Interfaces / *42.14*
42.8 MLL Prospects / *42.15*
42.9 Summary / *42.17*
42.10 Acknowledgments / *42.17*
42.11 References / *42.18*

Chapter 43. Polarizing Crystal Optics *Qun Shen* 43.1

43.1 Introduction / *43.1*
43.2 Linear Polarizers / *43.2*
43.3 Linear Polarization Analyzers / *43.4*
43.4 Phase Plates for Circular Polarization / *43.5*
43.5 Circular Polarization Analyzers / *43.6*
43.6 Acknowledgments / *43.8*
43.7 References / *43.8*

SUBPART 5.3. REFLECTIVE OPTICS

Chapter 44. Image Formation with Grazing Incidence Optics *James E. Harvey* 44.3

44.1 Glossary / *44.3*
44.2 Introduction to X-Ray Mirrors / *44.3*
44.3 Optical Design and Residual Aberrations of Grazing Incidence Telescopes / *44.6*
44.4 Image Analysis for Grazing Incidence X-Ray Optics / *44.12*
44.5 Validation of Image Analysis for Grazing Incidence X-Ray Optics / *44.16*
44.6 References / *44.18*

Chapter 45. Aberrations for Grazing Incidence Optics *Timo T. Saha* 45.1

45.1 Grazing Incidence Telescopes / *45.1*
45.2 Surface Equations / *45.1*
45.3 Transverse Ray Aberration Expansions / *45.3*
45.4 Curvature of the Best Focal Surface / *45.5*
45.5 Aberration Balancing / *45.5*
45.6 On-Axis Aberrations / *45.6*
45.7 References / *45.8*

SPERO EX. 2060

Chapter 46. X-Ray Mirror Metrology *Peter Z. Takacs* 46.1

46.1 Glossary / *46.1*
46.2 Introduction / *46.1*
46.3 Surface Finish Metrology / *46.2*
46.4 Surface Figure Metrology / *46.3*
46.5 Practical Profile Analysis Considerations / *46.6*
46.6 References / *46.12*

Chapter 47. Astronomical X-Ray Optics *Marshall K. Joy and Brian D. Ramsey* 47.1

47.1 Introduction / *47.1*
47.2 Wolter X-Ray Optics / *47.2*
47.3 Kirkpatrick-Baez Optics / *47.7*
47.4 Hard X-Ray Optics / *47.9*
47.5 Toward Higher Angular Resolution / *47.10*
47.6 References / *47.11*

Chapter 48. Multifoil X-Ray Optics *Ladislav Pina* 48.1

48.1 Introduction / *48.1*
48.2 Grazing Incidence Optics / *48.1*
48.3 Multifoil Lobster-Eye Optics / *48.2*
48.4 Multifoil Kirkpatrick-Baez Optics / *48.3*
48.5 Summary / *48.4*
48.6 References / *48.4*

Chapter 49. Pore Optics *Marco W. Beijersbergen* 49.1

49.1 Introduction / *49.1*
49.2 Glass Micropore Optics / *49.1*
49.3 Silicon Pore Optics / *49.6*
49.4 Micromachined Silicon / *49.7*
49.5 References / *49.7*

Chapter 50. Adaptive X-Ray Optics *Ali Khounsary* 50.1

50.1 Introduction / *50.1*
50.2 Adaptive Optics in X-Ray Astronomy / *50.2*
50.3 Active and Adaptive Optics for Synchrotron- and Lab-Based X-Ray Sources / *50.2*
50.4 Conclusions / *50.8*
50.5 References / *50.8*

Chapter 51. The Schwarzschild Objective *Franco Cerrina* 51.1

51.1 Introduction / *51.1*
51.2 Applications to X-Ray Domain / *51.3*
51.3 References / *51.5*

Chapter 52. Single Capillaries *Donald H. Bilderback and Sterling W. Cornaby* 52.1

52.1 Background / *52.1*
52.2 Design Parameters / *52.1*
52.3 Fabrication / *52.4*
52.4 Applications of Single-Bounce Capillary Optics / *52.5*
52.5 Applications of Condensing Capillary Optics / *52.6*
52.6 Conclusions / *52.6*

SPERO EX. 2060

52.7 Acknowledgments / *52.6*
52.8 References / *52.6*

Chapter 53. Polycapillary X-Ray Optics *Carolyn MacDonald and Walter Gibson* 53.1

53.1 Introduction / *53.1*
53.2 Simulations and Defect Analysis / *53.3*
53.3 Radiation Resistance / *53.5*
53.4 Alignment and Measurement / *53.5*
53.5 Collimation / *53.8*
53.6 Focusing / *53.9*
53.7 Applications / *53.10*
53.8 Summary / *53.19*
53.9 Acknowledgments / *53.19*
53.10 References / *53.19*

SUBPART 5.4. X-RAY SOURCES

Chapter 54. X-Ray Tube Sources *Susanne M. Lee and Carolyn MacDonald* 54.3

54.1 Introduction / *54.3*
54.2 Spectra / *54.4*
54.3 Cathode Design and Geometry / *54.10*
54.4 Effect of Anode Material, Geometry, and Source Size on Intensity and Brightness / *54.11*
54.5 General Optimization / *54.15*
54.6 References / *54.17*

Chapter 55. Synchrotron Sources *Steven L. Hulbert and Gwyn P. Williams* 55.1

55.1 Introduction / *55.1*
55.2 Theory of Synchrotron Radiation Emission / *55.2*
55.3 Insertion Devices (Undulators and Wigglers) / *55.9*
55.4 Coherence of Synchrotron Radiation Emission in the Long Wavelength Limit / *55.17*
55.5 Conclusion / *55.20*
55.6 References / *55.20*

Chapter 56. Laser-Generated Plasmas *Alan Michette* 56.1

56.1 Introduction / *56.1*
56.2 Characteristic Radiation / *56.2*
56.3 Bremsstrahlung / *56.8*
56.4 Recombination Radiation / *56.10*
56.5 References / *56.10*

Chapter 57. Pinch Plasma Sources *Victor Kantsyrev* 57.1

57.1 Introduction / *57.1*
57.2 Types of Z-Pinch Radiation Sources / *57.2*
57.3 Choice of Optics for Z-Pinch Sources / *57.4*
57.4 References / *57.5*

Chapter 58. X-Ray Lasers *Greg Tallents* 58.1

58.1 Free-Electron Lasers / *58.1*
58.2 High Harmonic Production / *58.2*
58.3 Plasma-Based EUV Lasers / *58.2*
58.4 References / *58.4*

SPERO EX. 2060

Chapter 59. Inverse Compton X-Ray Sources *Frank Carroll* 59.1

59.1 Introduction / *59.1*
59.2 Inverse Compton Calculations / *59.2*
59.3 Practical Devices / *59.2*
59.4 Applications / *59.3*
59.5 Industrial/Military/Crystallographic Uses / *59.4*
59.6 References / *59.4*

SUBPART 5.5. X-RAY DETECTORS

Chapter 60. Introduction to X-Ray Detectors *Walter Gibson and Peter Siddons* 60.3

60.1 Introduction / *60.3*
60.2 Detector Type / *60.3*
60.3 Summary / *60.9*
60.4 References / *60.10*

Chapter 61. Advances in Imaging Detectors *Aaron Couture* 61.1

61.1 Introduction / *61.1*
61.2 Flat-Panel Detectors / *61.3*
61.3 CCD Detectors / *61.7*
61.4 Conclusion / *61.8*
61.5 References / *61.8*

Chapter 62. X-Ray Spectral Detection and Imaging *Eric Lifshin* 62.1

62.1 References / *62.6*

SUBPART 5.6. NEUTRON OPTICS AND APPLICATIONS

Chapter 63. Neutron Optics *David Mildner* 63.3

63.1 Neutron Physics / *63.3*
63.2 Scattering Lengths and Cross Sections / *63.5*
63.3 Neutron Sources / *63.12*
63.4 Neutron Optical Devices / *63.15*
63.5 Refraction and Reflection / *63.19*
63.6 Diffraction and Interference / *63.23*
63.7 Polarization Techniques / *63.27*
63.8 Neutron Detection / *63.31*
63.9 References / *63.35*

Chapter 64. Grazing-Incidence Neutron Optics *Mikhail Gubarev and Brian Ramsey* 64.1

64.1 Introduction / *64.1*
64.2 Total External Reflection / *64.1*
64.3 Diffractive Scattering and Mirror Surface Roughness Requirements / *64.2*
64.4 Imaging Focusing Optics / *64.3*
64.5 References / *64.7*

Index I.1

SPERO EX. 2060

where N represents molecular packing density, p is the molecular length-to-width (w) ratio, $J \cong J_o S$ is the Maier-Saupe mean-field coupling constant; k is the Boltzmann constant, T is the Kelvin temperature, S and P_4 are the nematic order parameters of the second and fourth order, respectively, and Λ is the friction coefficient of LC:

$$\Lambda \cong 100\ (1 - \Phi) N^2 w^6 p^{-2}\ [(kT)^5/G^3]\ (I_\perp/kT)^{1/2} \cdot \exp\ [3(G + I_o)/kT] \tag{21}$$

where Φ is the volume fraction of molecules ($\Phi = 0.5$ to 0.6 for dense molecular liquids), $G >> I_o$ is the isotropic intermolecular attraction energy, and $I_\perp$ and I_o are the inertia tensors.

From the above analysis, the parameters affecting the rotational viscosity of a LC are[53]

1. Activation energy ($E_a \sim 3G$): a LC molecule with low activation energy leads to a low viscosity.
2. Moment of inertia: a LC molecule with linear shape and low molecular weight would possess a small moment of inertia and exhibit a low viscosity.
3. Inter-molecular association: a LC with weak inter-molecular association, for example, not form dimer, would reduce the viscosity significantly.
4. Temperature: elevated temperature operation of a LC device may be the easiest way to lower viscosity. However, birefringence, elastic, and dielectric constants are all reduced as well.

8.6 LIQUID CRYSTAL CELLS

Three kinds of LC cells have been widely used for display applications. They are (1) twisted-nematic (TN) cell, (2) in-plane switching (IPS) cell, and multidomain vertical alignment (MVA) cell. For phase-only modulation, homogeneous cell is preferred. The TN cell dominates notebook market because of its high transmittance and low cost. However, its viewing angle is limited. For wide-view applications, for example, LCD TVs, optical film-compensated IPS and MVA are the two major camps. In this section, we will discuss the basic electro-optics of TN, IPS, and MVA cells.

Twisted-Nematic (TN) Cell

The first liquid crystal displays that became successful on the market were the small displays in digital watches. These were simple twisted nematic (TN) devices with characteristics satisfactory for such simple applications.[19] The basic operation principals are shown in Fig. 21. In the TN display, each LC cell consists of a LC material sandwiched between two glass plates separated by a gap of 5 to 8 μm.

The inner surfaces of the plates are deposited with transparent electrodes made of conducting coatings of indium tin oxide (ITO). These transparent electrodes are overcoated with a thin layer of polyimide with a thickness of about 80 angstroms. The polyimide films are unidirectional rubbed with the rubbing direction of the lower substrate perpendicular to the rubbing direction of the upper surface. Thus, in the inactivated state (voltage OFF), the local director undergoes a continuous twist of 90° in the region between the plates. Sheet polarizers are laminated on the outer surfaces of the plates. The transmission axes of the polarizers are aligned parallel to the rubbing directions of the adjacent polyimide films. When light enters the cell, the first polarizer lets through only the component oscillating parallel to the LC director next to the entrance substrate. During the passage through the cell, the polarization plane is turned along with the director helix, so that when the light wave arrives at the exit polarizer, it passes unobstructed. The cell is thus transparent in the OFF state; this mode is called normally white (NW).

Figure 22 depicts the normalized voltage-dependent light transmittance ($T_\perp$) of the 90° TN cell at three primary wavelengths: $R = 650$ nm, $G = 550$ nm, and $B = 450$ nm. Since human eye has the greatest

SPERO EX. 2060

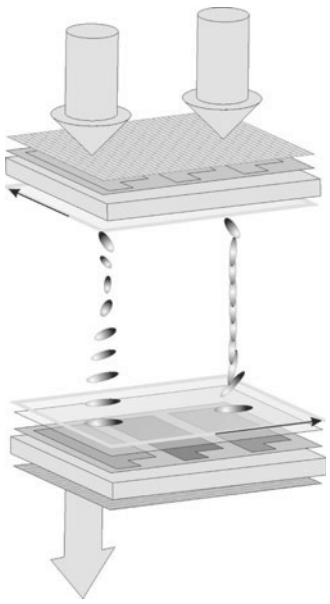

FIGURE 21 The basic operation principles of the TN cell.

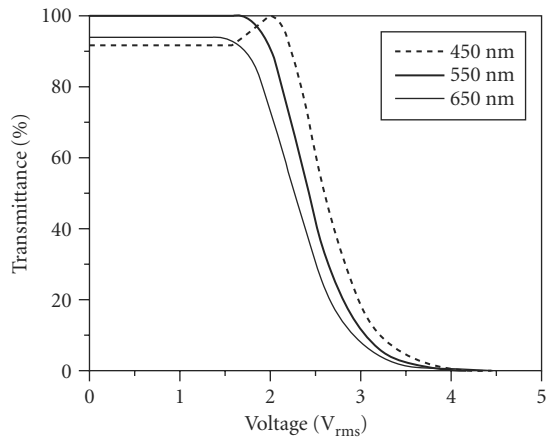

FIGURE 22 Voltage-dependent transmittance of a normally white 90° TN cell. $d\Delta n = 480$ nm.

sensitivity at green, we normally optimize the cell design at $\lambda \sim 550$ nm. To meet the Gooch-Tarry first minimum condition, for example, $d\Delta n = (\sqrt{3}/2)\lambda$, the employed cell gap is 5-μm and the LC birefringence is $\Delta n \sim 0.096$. From Fig. 22, the wavelength effect on the transmittance at V = 0 is within 8 percent. Therefore, the TN cell can be treated as an "achromatic" half-wave plate.

The response time of a TN LCD depends on the cell gap and the γ_1/K_{22} of the LC mixture employed. For a 5-μm cell gap, the optical response time is ~30 to 40 ms. At V = 5 V_{rms}, the contrast ratio (CR) reaches ~500:1. These performances, although not perfect, are acceptable for notebook computers. A major drawback of the TN cell is its narrow viewing angle and grayscale inversion originated from the LC directors tilting out of the plane. Because of this molecular tilt, the viewing angle in the vertical direction is narrow and asymmetric, and has grayscale inversion.[54] Despite a relatively slow switching time and limited viewing angle, the TN cell is still widely used for many applications because of its simplicity and low cost. Recently, a fast-response (~2 ms gray-to-gray response time) TN notebook computer has been demonstrated by using a thin cell gap (2 μm), low viscosity LC mixture, and overdrive and undershoot voltage method.

In-Plane Switching (IPS) Cell

In an IPS cell, the transmission axis of the polarizer is parallel to the LC director at the input plane.[55] The optical wave traversing through the LC cell is an extraordinary wave whose polarization state remains unchanged. As a result, a good dark state is achieved since this linearly polarized light is completely absorbed by the crossed analyzer. When an electric field is applied to the LC cell, the LC directors are reoriented toward the electric field (along the y axis). This leads to a new director distribution with a twist $f(z)$ in the xy plane as Fig. 23 shows.

Figure 24 depicts the voltage-dependent light transmittance of an IPS cell. The LC employed is MLC-6686, whose $\Delta\varepsilon = 10$ and $\Delta n = 0.095$, the electrode width is 4 μm, electrode gap 8 μm, and cell

SPERO EX. 2060

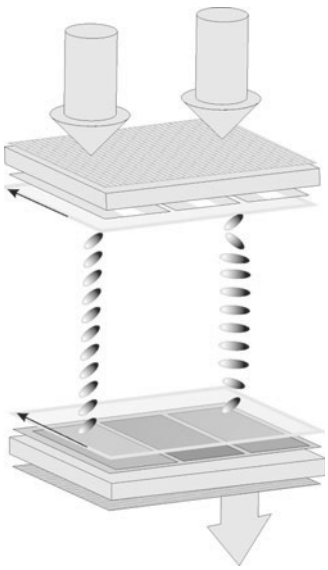

FIGURE 23 IPS mode LC display.

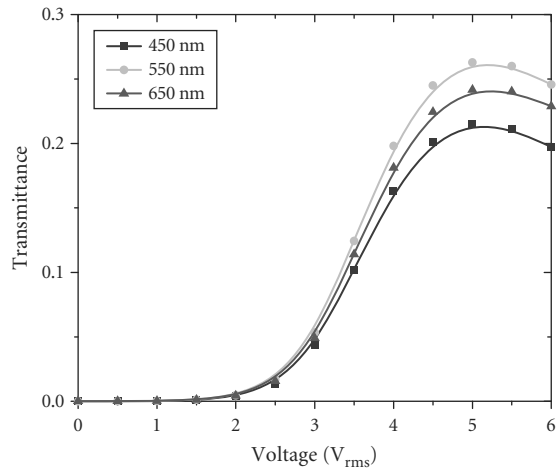

FIGURE 24 Voltage-dependent light transmittance of the IPS cell. LC: MLC-6686, $\Delta\varepsilon = 10$, electrode width = 4 μm, gap = 8 μm, and cell gap $d = 3.6$ μm.

gap $d = 3.6$ μm. The threshold voltage occurs at $V_{th} \sim 1.5\ V_{rms}$ and maximum transmittance at ~5 V_{rms} for both wavelengths. Due to absorption, the maximum transmittance of the two polarizers (without LC cell) is 35.4, 33.7, and 31.4 percent for RGB wavelengths, respectively.

Vertical Alignment (VA) Cell

The vertically aligned LC cell exhibits an unprecedentedly high contrast ratio among all the LC modes developed.[56] Moreover, its contrast ratio is insensitive to the incident light wavelength, cell thickness, and operating temperature. In principle, in voltage-OFF state the LC directors are perpendicular to the cell substrates, as Fig. 25 shows. Thus, its contrast ratio at normal angle is limited by the crossed polarizers. Application of a voltage to the ITO electrodes causes the directors to tilt away from the normal to the glass surfaces. This introduces birefringence and subsequently light transmittance because the refractive indices for the light polarized parallel and perpendicular to the directors are different.

Figure 26 shows the voltage-dependent transmittance of a VA cell with $d\Delta n = 350$ nm between two crossed polarizers. Here, a single domain VA cell employing Merck high resistivity MLC-6608 LC mixture is simulated. Some physical properties of MLC-6608 are listed as follows: $n_e = 1.562$, $n_o = 1.479$ (at $\lambda = 546$ nm and $T = 20°C$); clearing temperature $T_c = 90°C$; $\Delta\varepsilon = -4.2$, and rotational viscosity $\gamma_1 = 186$ mPas at 20°C.

From Fig. 26, an excellent dark state is obtained at normal incidence. As the applied voltage exceeds the Freederickz threshold voltage ($V_{th} \sim 2.1\ V_{rms}$), LC directors are reoriented by the applied electric field resulting in light transmission from the crossed analyzer. From the figure, RGB wavelengths reach their peak at different voltages, blue at ~4 V_{rms}, and green at ~6 V_{rms}. The on-state dispersion is more forgiven than the dark state. A small light leakage in the dark state would degrade the contrast ratio significantly, but less noticeable from the bright state.

It should be mentioned that in Figs. 25 and 26 only a single domain is considered, thus, its viewing angle is quite narrow. To achieve wide view, four domains with film compensation are required. Several approaches, such as Fujitsu's MVA (multidomain VA) and Samsung's PVA (Patterned VA),

SPERO EX. 2060

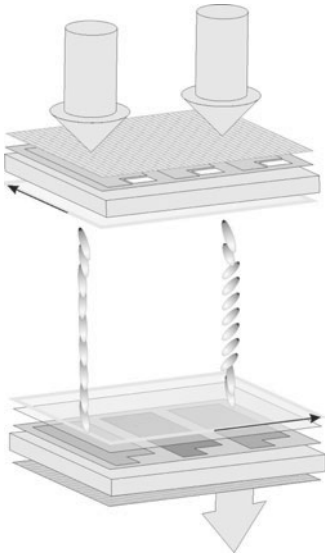

FIGURE 25 VA mode LC display.

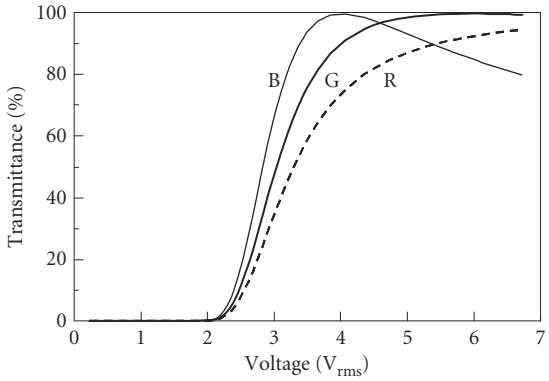

FIGURE 26 Voltage-dependent normalized transmittance of a VA cell. LC: MLC-6608. $d\Delta n$ = 350 nm. R = 650 nm, G = 550 nm, and B = 450 nm.

have been developed for obtaining four complementary domains. Figure 27 depicts the PVA structure developed by Samsung.

As shown in Fig. 27, PVA has no pretilt angle. The four domains are induced by the fringe electric fields. On the other hand, in Fujitsu's MVA, physical protrusions are used to provide initial pretilt direction for forming four domains. The protrusions not only reduce the aperture ratio but also cause light leakage in the dark state because the LCs on the edges of protrusions are tilted so that they exhibit birefringence. It would be desirable to eliminate protrusions for MVA and create a pretilt angle in each domain for both MVA and PVA to guide the LC reorientation direction. Based on this concept, surface polymer sustained alignment (PSA) technique has been developed.[57] A very small percentage (~0.2 wt %) of reactive mesogen monomer and photoinitiator are mixed in a negative $\Delta\varepsilon$ LC host and injected into a LCD panel. While a voltage is applied to generate four domains, a UV light is used to cure the monomers. As a result, the monomers are adsorbed onto the surfaces. These cured polymers, although in low density, will provide a pretilt angle within each domain to guide the LC reorientation. Thus, the rise time is reduced by nearly 2× while the decay time remains more or less unchanged.[58]

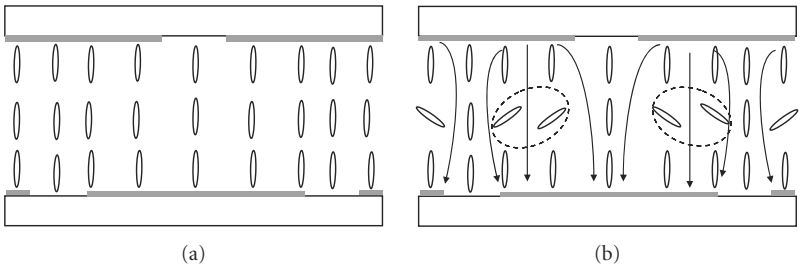

FIGURE 27 (*a*) LC directors of PVA at V = 0 and (*b*) LC directors of PVA at a voltage-on state. The fringe fields generated by the top and bottom slits create two opposite domains in this cross section. When the zigzag electrodes are used, four domains are generated.

SPERO EX. 2060

8.7 LIQUID CRYSTALS DISPLAYS

The most common and well recognized applications of liquid crystals nowadays are displays. It is the most natural way to utilize extraordinary electro-optical properties of liquid crystals together with its liquid-like behavior. All the other applications are called as nondisplay applications of liquid crystals. Nondisplay applications are based on the liquid crystals molecular order sensitivity to the external incentive. This can be an external electric and magnetic field, temperature, chemical agents, mechanical stress, pressure, irradiation by different electromagnetic wave, or radioactive agents. Liquid crystals sensitivity for such wide spectrum of factors results in tremendous diversity of nondisplay applications. It starts from spatial light modulators for laser beam steering, adaptive optics through telecommunication area (light shutters, attenuators, and switches), cholesteric LC filters, LC thermometers, stress meters, dose meters to ends up with liquid crystals paints, and cosmetics. Another field of interest employing lyotropic liquid crystals is biomedicine where it plays an important role as a basic unit of the living organisms by means of plasma membranes of the living cells. More about existing nondisplays applications can be found in preferred reading materials.

Three types of liquid crystal displays (LCDs) have been developed: (1) transmissive, (2) reflective, and (3) transflective. Each one has its own unique properties. In the following sections, we will introduce the basic operation principles of these display devices.

Transmissive TFT LCDs

A transmissive LCD uses a backlight to illuminate the LCD panel to achieve high brightness (300 to 500 nits) and high contrast ratio (>2000:1). Some transmissive LCDs, such as twisted-nematic (TN), do not use phase compensation films or multidomain structures so that their viewing angle is limited and they are more suitable for single viewer applications, for example, mobile displays and notebook computers. With phase compensation films and multidomain structures, the direct-view transmissive LCDs exhibit a wide viewing angle and high contrast ratio, and have been widely used for desktop computers and televisions. However, the cost of direct-view large screen LCDs is still relatively expensive. To obtain a screen diagonal larger than 2.5 m, projection displays, such as data projector, using transmissive microdisplays are still a favorable choice. There, a high power arc lamp or light emitting diode (LED) arrays are used as light source. Using a projection lens, the displayed image is magnified by more than 50×. To reduce the size of optics and cost, the LCD panel is usually made small (<25 mm in diagonal) and each pixel size is ~20 to 40 μm. Thus, poly-silicon-based TFT LCD is the common choice.

Figure 28 shows the device structure of a transmissive thin-film-transistor (TFT) LCD using amorphous silicon (a-Si) transistors. LCD is a nonemissive display, that is, it does not emit light, instead, it functions as a two-dimensional spatial light modulator. Thus, a backlight is needed. A diffuser is used to homogenize the backlight in order to avoid hot spots. Some optical films are stacked to steer the Lambertian backlight to the central ±40° for improving display brightness. Since most LCDs require a linearly polarized light in order to obtain a high contrast ratio, two sheets of stretched dichroic polarizers are used for large size direct-view displays. The first glass substrate contains TFT arrays, which serve as independent light switches. Each display pixel is controlled by a TFT. Since TFT is sensitive and should be shielded from backlight illumination, the actual aperture ratio (the transparent ITO electrode area) is reduced to ~80 percent, depending on the pixel density. As the pixel density increases, the aperture ratio decreases. The LC layer is sandwiched between two ITO substrates whose inner surface is coated with a thin (80 to 100 nm) polyimide layer. Some LCDs (twisted-nematic, in-plane switching and fringe field switching) require rubbing but some (multidomain vertical alignment and patterned vertical alignment) do not. The cell gap is usually controlled at ~3.5 to 4.0 μm for a transmissive LCD. The performance of the display such as light throughput, response time, and viewing angle are all influenced by the LC configuration employed.

For direct-view LCDs, compact size, lightweight, and low power consumption are equally important as viewing angle, color, and contrast ratio. For direct-view LCDs, color filters are embedded in the inner side of the top (second) substrate. Three subpixels (red, green, and blue) form a color pixel. The size of

SPERO EX. 2060

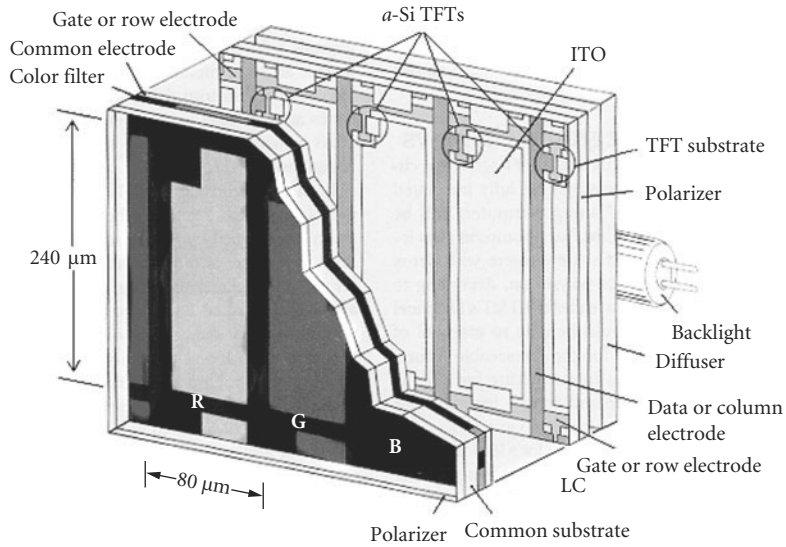

FIGURE 28 Device structure of a color pixel of a transmissive TFT LCD.

each subpixel is ~80 μm × 240 μm. Each subpixel transmits only one color; the other colors are absorbed. Figure 29 depicts the emission spectra of a backlight (cold cathode fluorescent lamp, CCFL) and RGB light emitting diodes (LEDs), and the transmission spectra of RGB color filters.

From Fig. 29, the transmission spectra of RGB color filters are relatively broad. The advantage is to transmit more light however its color purity is degraded. The peak transmission of the RGB color filters is ~70, 80, and 90 percent, respectively. Roughly speaking, each color filter only transmits ~25 percent of the incident white light. The rest ~75 percent is absorbed by the color pigments. Moreover, CCFL emits two unwanted lines: blue-green (~480 nm) and orange (~580 nm). The blue-green light will transmit through the blue and green color filters simultaneously. Similarly, the orange light will transmit through the green and red color filters simultaneously. These leaked lights will downgrade the color purity (or color saturation) of the display. Therefore, the color gamut of a typical transmissive TFT LCD is ~75 percent of NTSC (National Television System Committee) standard. With improved CCFL spectra, the color gamut can reach ~92 percent. LEDs have narrower emission spectra that also match

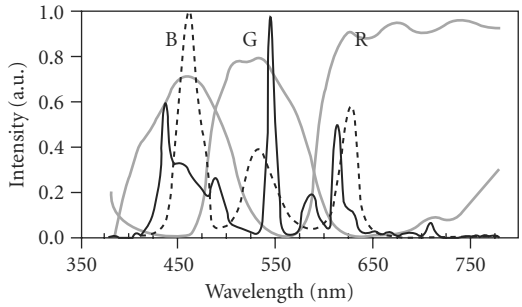

FIGURE 29 Transmission spectra of RGB color filters (thick gray lines), and emission spectra of CCFL backlight (thin black lines) and LEDs (dashed lines).

SPERO EX. 2060

better with the transmission spectra of the color filters, thus the color gamut reaches ~120 percent.[59] For a display device, a wider color gamut is not necessarily better; natural colors are also important. After all, display is an art where perception plays an important role.

After taking into account the optical losses from polarizers, color filters, and TFT aperture ratio, the overall system optical efficiency is about 6 to 7 percent for a direct-view LCD. If wide view technology is included,[60] the total light efficiency is decreased to ~5 percent. Low optical efficiency implies high power consumption and more heat generation inside the display chasse. For a thin LCD, thermal dissipation is a critical issue. For portable displays, low power consumption is desirable because it lengthens the battery operating hours. Several approaches have been developed to reduce power consumption, for example, polarization conversion of backlight[61] and two-dimensional LED backlight with local dimming capability.[62–64] The use of LED backlight offers several additional advantages such as wide color gamut, high dynamic contrast ratio (>50,000:1), ~2× reduction in power consumption, and fast turn-on and off times (~10 ns) for reducing the motion picture image blurs.[65] Some technological concerns are color and power drifting as the junction temperature changes, and cost.

Reflective LCDs

Figure 30 shows a device structure of a TFT-based reflective LCD. The top linear polarizer and a broadband quarter-wave film forms an equivalent crossed polarizer for the incident and exit beams. This is because the LC modes work better under crossed-polarizer condition. The bumpy reflector not only reflects but also diffuses the ambient light to the observer in order to avoid specular reflection and widen the viewing angle. This is a critical part for reflective LCDs. The TFT is hidden beneath the bumpy reflector, thus the R-LCD can have a large aperture ratio (~90%). The light blocking layer (LBL) is used to absorb the scattered light from neighboring pixels. Two popular LCD modes have been widely used for R-LCDs: (1) VA cell, and (2) mixed-mode twisted nematic (MTN) cell. The VA cell utilizes the phase retardation effect while the MTN cell uses the combination of polarization rotation and birefringence effects.

In a reflective LCD, there is no built-in backlight unit; instead, it utilizes ambient light for reading out the displayed images. In comparison to transmissive LCDs, reflective LCDs have advantages in lower power consumption, lighter weight, and better sunlight readability. However, a reflective LCD is inapplicable under low or dark ambient conditions. Therefore, the TFT-based reflective LCD is gradually losing its ground.

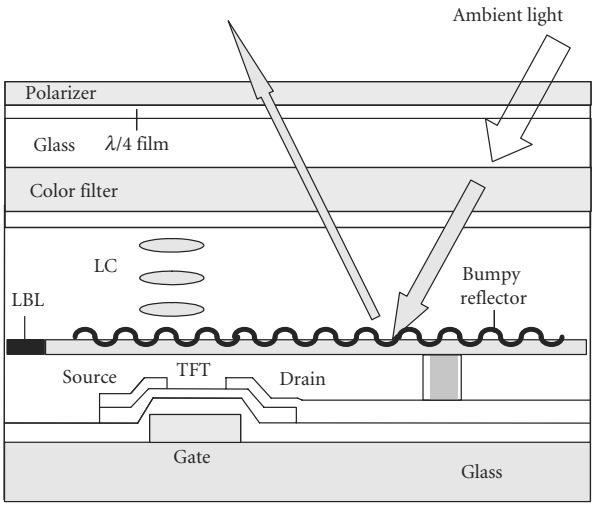

FIGURE 30 Device structure of a direct-view reflective LCD.

SPERO EX. 2060

Flexible reflective LCDs using cholesteric liquid crystal display (Ch-LCD) and bistable nematic are gaining momentum because they can be used as electronic papers. These reflective LCDs use ambient light to readout the displayed images. Ch-LCD has helical structure which reflects color so that the display does not require color filters, neither polarizer. Thus, the reflectance for a given color band which depends on the pitch length and refractive index of the employed LC is relatively high (~30%). Moreover, it does not require a backlight so that its weight is light and the total device thickness can be thinner than 200 μm. Therefore, it is a strong contender for color flexible displays. Ch-LCD is a bistable device so that its power consumption is low, provided that the device is not refreshed too frequently. A major drawback of a reflective direct-view LCD is its poor readability under low ambient light.

Another reflective LCD developed for projection TVs is liquid-crystal-on-silicon (LCoS) microdisplay. Unlike a transmissive microdisplay, LCoS is a reflective device. Here the reflector employed is an aluminum metallic mirror. Crystalline silicon has high mobility so that the pixel size can be made small (<10 μm) and aperture ratio >90 percent. Therefore, the image not only has high resolution but also is seamless. By contrast, a transmissive microdisplay's aperture ratio is about 65 percent. The light blocked by the black matrices show up in the screen as dark patterns (also known as screen door effect). Viewing angle of a LCD is less critical in projection than direct-view displays because in a projection display the polarizing beam splitter has a narrower acceptance angle than the employed LCD.

Transflective LCDs

In a transflective liquid crystal display (TR-LCD), a pixel is divided into two parts: transmissive (T) and reflective (R). The T/R area ratio can vary from 80/20 to 20/80, depending on the applications. In dark ambient the backlight is on and the display works as a transmissive one, while at bright ambient the backlight is off and only the reflective mode is operational.

Dual-Cell-Gap Transflective LCDs In a TR-LCD, the backlight traverses the LC layer once, but the ambient light passes through twice. As a result, the optical path length is unequal. To balance the optical path difference between the T and R regions for a TR-LCD, dual-cell-gap device concept is introduced. The basic requirement for a TR-LCD is to find equal phase retardation between the T and R modes, which is

$$d_T(\Delta n)_T = 2d_R(\Delta n)_R \tag{22}$$

If T and R modes have the same effective birefringence, then the cell gap should be different. This is the so-called dual cell gap approach. On the other hand, if the cell gap is uniform (single cell gap approach), then we should find ways to make $(\Delta n)_T = 2(\Delta n)_R$. Let us discuss the dual cell gap approaches first.

Figure 31*a* shows the schematic device configuration of a dual-cell-gap TR-LCD. Each pixel is divided into a reflective region with cell gap d_R and a transmissive region with cell gap d_T. The LC employed could be homogeneous alignment (also known as ECB, electrically controlled birefringence) or vertical alignment, as long as it is a phase retardation type. To balance the phase retardation between the single and double pass of the T and R parts, we could set $d_T = 2d_R$. Moreover, to balance the color saturation due to single and double-pass discrepancy, we could use thinner or holed color filters in the R part. The top quarter wave plate is needed mainly for the reflective mode to obtain a high contrast ratio. Therefore, in the T region, the optic axis of the bottom quarter-wave plate should be aligned perpendicular to that of the top one so that their phase retardations are canceled.

A thin homogeneous cell is difficult to find a good common dark state for RGB wavelengths without a compensation film.[55] The compensation film can be designed into the top quarter-wave film shown in Fig. 31*a* to form a single film. Here, let us take a dual cell gap TR-LCD using VA (or MVA for wide-view) and MLC-6608 ($\Delta\varepsilon = -4.2$, $\Delta n = 0.083$) as an example. We set $d_R = 2.25$ μm in the R region and $d_T = 4.5$ μm in the T region. Figure 31*b* depicts the voltage-dependent transmittance (VT) and reflectance (VR) curves at normal incidence. As expected, both VT and VR curves perfectly overlap with each other. Here $d_R\Delta n = 186.8$ nm and $d_T\Delta n = 373.5$ nm are intentionally designed to be larger than $\lambda/4$ (137.5 nm) and $\lambda/2$ (275 nm), respectively, in order to reduce the on-state voltage to ~5 V_{rms}.

SPERO EX. 2060

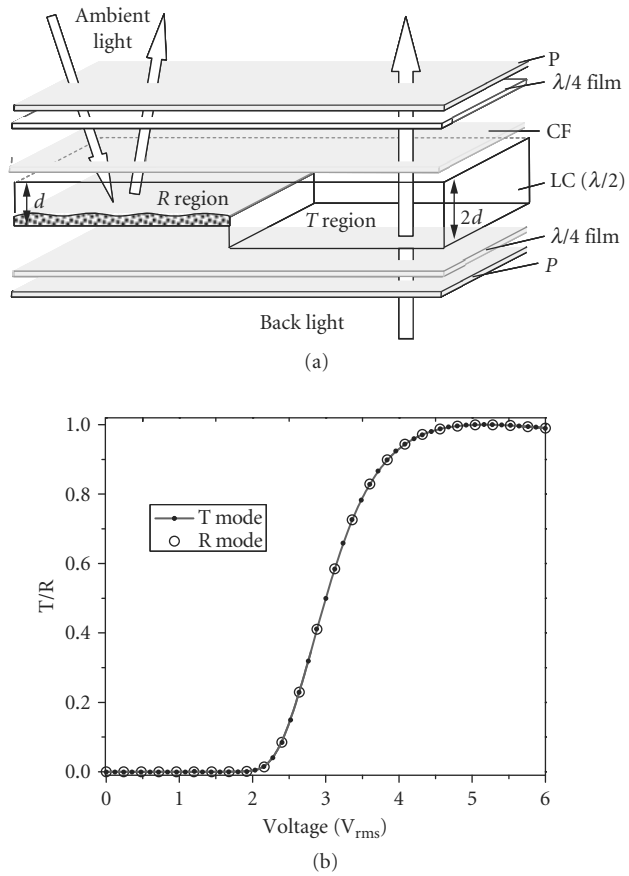

FIGURE 31 (*a*) Schematic device configuration of the dual-cell-gap TR-LCD. (*b*) Simulated VT and VR curves using VA (or MVA) cells. LC: MLC-6608, $dT = 4.5$ μm, $dR = 2.25$ μm, and $\lambda = 550$ nm.

Three problems of dual-cell-gap TR-LCDs are encountered: (1) Due to the cell gap difference the LC alignment is distorted near the T and R boundaries. The distorted LCs will cause light scattering and degrade the device contrast ratio. Therefore, these regions should be covered by black matrices in order to retain a good contrast ratio. (2) The thicker cell gap in the T region results in a slower response time than the R region. Fortunately, the dynamic response requirement in mobile displays is not as strict as those for video applications. This response time difference, although not perfect, is still tolerable. (3) The view angle of the single-domain homogeneous cell mode is relatively narrow because the LC directors are tilted out of the plane by the longitudinal electric field. To improve view angle, a biaxial film[66] or a hybrid aligned nematic polymeric film[67] is needed. Because the manufacturing process is compatible with the LCD fabrication lines, the dual-cell-gap TR-LCD is widely used in commercial products, such as iPhones.

Single-Cell-Gap Transflective LCDs As its name implies, the single-cell-gap TR-LCD has a uniform cell gap in the T and R regions. Therefore, we need to find device concepts to achieve $(\Delta n)_T = 2(\Delta n)_R$. Several approaches have been proposed to solve this problem. In this section, we will discuss two

SPERO EX. 2060

examples: (1) dual-TFT method in which one TFT is used to drive the T mode and another TFT to drive the R mode at a lower voltage,[68] and (2) divided-voltage method:[69] to have multiple R parts and the superimposed VR curve matches the VT curve.

Example 3: Dual-TFT Method Figure 32*a* shows the device structure of a TR-LCD using two TFTs to separately control the gamma curves of the T and R parts. Here, TFT-1 is connected to the bumpy reflector and TFT-2 is connected to the ITO of the transmissive part. Because of the double passes, the VR curve has a sharper slope than the VT curve and it reaches the peak reflectance at a lower voltage, as shown in Fig. 32*b*. Let us use a 4.5-μm vertically aligned LC layer with 88° pretilt angle as an example. The LC mixture employed is Merck MLC-6608 and wavelength is $\lambda = 550$ nm. From Fig. 32*b*, the peak reflectance occurs at 3 V_{rms} and transmittance at 5.5 V_{rms}. Thus, the maximum voltage of TFT-1 should be set at 5.5 V and TFT-2 at 3 V. This driving scheme is also called double-gamma method.[70] The major advantage of this dual-TFT approach is its simplicity. However, each TFT takes up some real estate so that the aperture ratio for the T mode is reduced.

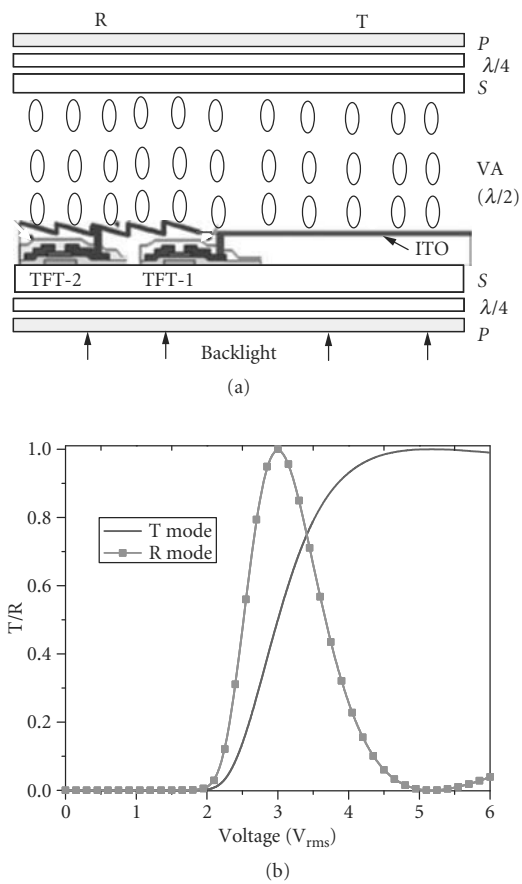

FIGURE 32 (*a*) Device structure of a dual-TFT TR-LCD and (*b*) simulated VT and VR curves using a 4.5-μm, MLC-6608 LC layer.

SPERO EX. 2060

For a TR-LCD, the T mode should have priority over R mode. The major function of R mode is to preserve sunlight readability. In general, the viewing angle, color saturation, and contrast ratio of R mode are all inferior to T mode. In most lighting conditions except under direct sunlight, T mode is still the primary display.

Example 4: Divided-Voltage Method Figure 33*a* shows the device structure of a TR-LCD using divided voltage method.[71] The R region consists of two sub-regions: R-I and R-II. Between R-II and bottom ITO, there is a passivation layer to weaken the electric field in the R-II region. As plotted in Fig. 33*b*, the VR-II curve in the R-II region has a higher threshold voltage than the VT curve due to this voltage shielding effect. To better match the VT curve, a small area in the T region is also used for R-I. The bumpy reflector in the R-I region is connected to the bottom ITO through a channeled electrode. Because of the double passes of ambient light, the VR-I curve is sharper than the VT curve. By properly choosing the R-I and R-II areas, we can match the VT and VR curves well, as shown in Fig. 33*b*.

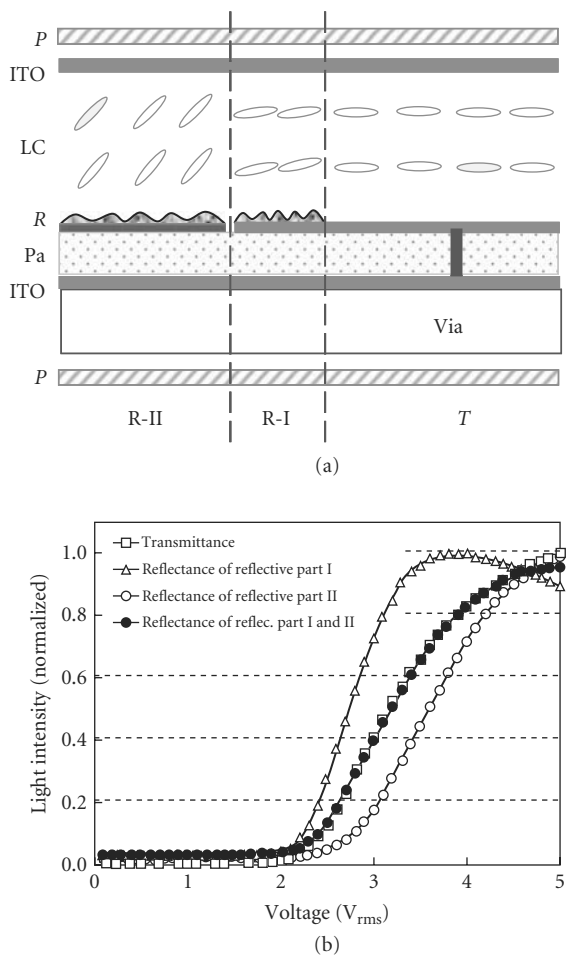

FIGURE 33 A transflective LCD using divided-voltage approach. (*a*) Device structure and (*b*) VT and VR curves at different regions. Here, *P*: polarizer, *R*: bumpy reflector, and Pa: passivation layer. (*Redrawn from Ref. 71.*)

SPERO EX. 2060